Detailed analysis of species production from the pyrolysis of the Phenolic Impregnated Carbon Ablator

Hsi-Wu Wong[a,*], Jay Peck[b], James Assif[b], Francesco Panerai[c], Jean Lachaud[d], Nagi N. Mansour[e]

[a]*Department of Chemical Engineering*
University of Massachusetts Lowell, Lowell, MA 01854
[b]*Center for Aero-Thermodynamics*
Aerodyne Research, Inc., Billerica, MA 01821
[c]*AMA Inc. at NASA Ames Research Center, Moffett Field, CA 94035*
[d]*Silicon Valley Initiatives*
University of California at Santa Cruz, Moffett Field, CA 94035
[e]*NASA Ames Research Center, Moffett Field, CA 94035*

Abstract

Many modern materials that are being developed to protect space vehicles entering planetary atmospheres use phenolic impregnated carbon fiber substrates as the basic material architecture. To mitigate the heat flux into the material, the decomposition of phenolic phase generates protective gases that blow into the boundary layer and help shield the material. The goal of this paper is to measure the decomposition products of cross-linked phenolic as used in NASA's Phenolic Impregnated Carbon Ablator (PICA). A custom batch reactor was designed to quantitatively determine detailed species production from the pyrolysis of PICA. A step-wise heating procedure using 50 K increments from room temperature up to 1250 K was followed. An initial PICA mass of 100 mg was loaded in the reactor, and the mass loss was

*Corresponding author
Email address: HsiWu_Wong@uml.edu (Hsi-Wu Wong)

measured after each 50 K step. Species production after each step was quantified using gas-chromatography techniques. The quantitative molar yields of pyrolysis products as a function of reaction temperature are compared to those from resole phenol-formaldehyde resin pyrolysis reported in the literature. The differences in product distributions between PICA pyrolysis and resole phenol-formaldehyde pyrolysis confirm that the decomposition products are sensitive to the composition of the material and the cross-linking process. These results indicate that characterizations need to be performed for all variations of phenolic-matrix based ablators. Such information is also critical for the development of next generation material response models.
Keywords: Pyrolysis; reaction kinetics; species production; PICA; thermal protection system

1. Introduction

Thermal Protection System (TPS) materials are used to protect space vehicles from aerodynamic heating during atmospheric reentry. Among many material architectures used in exploration vehicles, low-density carbon/resin (C/R) ablators represent a consolidated material choice for the heat shield of planetary exploration missions. Ablators within this class are typically made of a carbon fiber preform impregnated with phenol-formaldehyde resins. The Phenolic Impregnated Carbon Ablator (PICA), a low-density C/R ablator designed by NASA, has been successfully used on the Startdust [1] mission and later adopted as the heat shield material for the Mars Science Laboratory (MSL). PICA-X, a variant of PICA developed by SpaceX [2], has also

been successfully employed to protect the Dragon capsule. Concurrently, the European Space Agency is supporting the development of ASTERM, a lightweight ablator similar to PICA that could be used for sample return missions [3].

The design of ablative TPS critically relies upon material response modeling. While design codes are effective tools for TPS sizing during mission development phases, high fidelity material response models [4–8] can be used to simulate more detailed physical processes, and can be exercised during post-flight analyses to better understand discrepancies between flight data and simulation predictions. Dedicated fundamental experiments are being conducted to obtain accurate data for high-fidelity model developments and improved material response predictions [9–12].

During atmospheric entry, low-density C/R ablative materials undergo thermal degradation and ultimately recession. Various physical and chemical phenomena are involved in the ablation process, and the overall material response can be described by three steps [6, 7]: decomposition of solid resin via pyrolysis, transport of pyrolysis gases through porous char, and surface recession mainly via oxidation of carbonaceous phases. Other phenomena, including thermal and oxidative transport and mechanical material removal, are also important. In terms of simulating the pyrolysis of the solid resin, two quantities are usually needed from experiments: the chemical composition (speciation) and the rate of production of the pyrolysis products. Practical models to date use (1) data obtained from early experiments performed in the sixties for neat phenol-formaldehyde resin pyrolysis [13–20] or (2) equilibrium composition based on an estimated elementary composition [4, 5]. To

advance the development of high-fidelity material response models, there is a need for modern data obtained from refined experiments and state-of-the-art measurement techniques on the actual materials of interest.

In a previous study, we determined the detailed species production from the pyrolysis of a resole type phenol-formaldehyde (PF) resin at different temperatures [10, 11], allowing the consolidation of a suitable approach for quantifying resin decomposition data. Our experiments showed that pyrolysis of PF resin follows the three step degradation process proposed by Trick et al. [18, 19], where water is formed below a reaction temperature of 800 K, followed by volatile species (phenol derivatives and aromatics) production between 500–850 K and production of permanent gases between 800–1200 K.

In contrast to neat PF resin pyrolysis, very limited data are available on the pyrolysis of PICA. The work of Bessire et al. [9] documented species production from PICA pyrolysis. A sample of PICA was placed in a vacuum chamber and heated in the range of 373–1208 K by Joule heating, flowing electric current through the material. Mass spectral measurements were taken in-situ to avoid secondary reactions. The temperature-dependent product evolution was sketched and found to be consistent with earlier descriptions of three pyrolysis stages. The work, however, did not detect the production of hydrogen gas, which has been identified to be an important product at high ($>$ 800 K) reaction temperatures [10, 11, 14, 18, 19]. Quantification of absolute product yields from the pyrolysis reactions was also not performed.

In this work, we report data for quantitative species production from PICA pyrolysis obtained following the same experimental protocol previously

used for PF resin pyrolysis [10, 11]. Our experimental techniques combine batch reactions with mass spectrometry and gas chromatography analysis, enabling identification and quantification of pyrolysis products, corroborated by mass balance.

2. Pyrolysis experiments

2.1. Reactor design

The batch reactor system used in our previous experiments [10, 11] to quantify pyrolysis products from a resole-type phenol-formaldehyde (PF) resin pyrolysis was employed in this study. The reactor system, shown in Figure 1, is made of a stainless steel assembly and a quartz reactor tube, taking advantage of its good thermal shock resistance. Two type K thermocouples (Omega Engineering, KMQSS-062U-12) are attached to monitor the temperatures of the sample and the ferrule between the quartz reactor and the stainless steel assembly, respectively. A pressure transducer (Omega Engineering, PX309-005A5V) is attached for monitoring real-time pressure of the reactor system. During the experiments, the quartz tube, loaded with PICA samples, was the only heated zone kept in a custom-made high-temperature furnace constructed with nichrome heating wires (McMaster-Carr, 8880K76) and castable ceramics (Cotronics, Rescor 750). The furnace temperature was controlled by a PID controller (Omega Engineering, CN742). The condenser was attached to the heated section via a transfer line and was maintained at low temperature in a liquid nitrogen bath. This design ensures that any light reaction products (< 400 g/mole) formed in the quartz reactor would be transported to the condenser driven by temperature gradients to minimize

secondary gas-phase reactions. Using this reactor configuration, comprehensive collection of reaction products over a desired reaction time can be achieved, providing quantitative results and mass balance closure.

2.2. PICA samples tested

In this work, PICA samples supplied by Fiber Materials Incorporated (FMI, Biddeford, ME, USA) were tested. PICA is made with a commercially available carbon preform (FiberForm®), also produced by FMI, and a phenolic resin (Durite® SC-1008) distributed by Hexion (Batesville, AR, USA). The manufacturing processes include phenolic impregnation, elevated temperature curing, and vacuum-oven drying at proprietary conditions. FiberForm is a network of rayon-based carbon fibers with diameters between 9 and 11 μm. The material has nearly orthotropic thermal properties, which also confers orthotropic properties upon PICA. A typical SC-1008 resin contains 0.6 to 2 weight percent of formaldehyde, 11 to 18 weight percent of phenol, and 20 to 25 weight percent of isopropyl alcohol as a solvent. PICA's density and porosity, nominally 0.274 g/cm^3 ± 10% and 0.8 ± 10%, can vary depending on the phenolic loading. The high variability is due to the non-uniformity of the preform.

2.3. Experimental procedure

The experimental procedure in this work followed a step-wise heating–quenching cycle in reaction temperature of every 50 K [10, 11]. The main goal was to store and analyze pyrolysis products within 50 K temperature increments (that is, between 320 and 370 K, 370 and 420 K, etc.) rather than attempting on-the-fly measurements, which are susceptible to sample

loss due to product condensation in the reactor and transfer lines. There are two advantages to this approach: (1) the mass of the samples can be measured at each step, avoiding the need of using a thermogravimetric analyzer where volatile vapors may condense in the system, and (2) the volatile pyrolysis products that condense on the wall of the reactor assembly can be comprehensively collected by liquid extraction and analyzed. Gas chromatography (GC) techniques were used to identify and quantify the pyrolysis gases produced from the reactions.

An typical experiment started with loading 100 mg of PICA samples in the quartz reactor. This amount was chosen to have a comparable phenolic content to previous experiments where 50 mg of neat resole PF resin were initially loaded [10, 11], since PICA is nearly composed of half phenolic resin and half carbon preform [21]. The reactor was then connected to a vacuum line via the extraction port of the reactor assembly to reduce the system pressure below 13.33 Pa (0.1 torr) to ensure any gas-phase species within is removed. The extraction port was then closed, and the quartz reactor was inserted into the furnace pre-set at a desired temperature. The sample was then reacted at the target temperature for one hour. During this one-hour period, on-the-fly pressure measurement by the transducer was conducted, providing real-time pressure monitoring. After the reaction, the quartz reactor was immediately quenched in a cold water bath back to room temperature, typically achieved within two minutes. The final reactor pressure was then recorded by the pressure transducer, providing an estimate of the total amount of phenolic pyrolysis products formed in the gas phase at room temperature, before the needle valve was opened for analyzing the pyrolysis products.

The pyrolysis products were detected by gas chromatography (GC). After the GC analysis, the reactor assembly was disassembled, and the quartz tube was immediately capped to avoid penetration of ambient air humidity in the sample. An electronic balance (Mettler Toledo Excellence Plus XP105) with a repeatability of 0.01 mg was used to measure the weight of the capped quartz tube for obtaining mass loss of the sample resulted from the pyrolysis reaction. The stainless steel sections of the reactor assembly were rinsed with dichloromethane and dried in an oven at 373 K for 30 minutes. The reactor system was then reassembled and the elementary procedure was repeated using the reacted sample left in the quartz tube, with the furnace temperature set 50 K higher than the previous run until a final reaction temperature of 1250 K. The entire step-wise procedure was repeated three times to confirm reproducibility, and standard deviations of the three experiments were used as the error bars in the figures.

2.4. Gas chromatography (GC) analysis

The same GC analytical procedure reported in our previous work [11] was followed to comprehensively identify and quantify any pyrolysis products with a molecular weight smaller than 400 g/mol. To quantify permanent gaseous species, 5-10 torr of pentane was added as an external standard after reactions. A 2 mL gas phase sample was injected into an Agilent 7820A GC equipped with a thermal conductivity detector (TCD) and a ShinCarbon ST 80/100 carbon column (Restek), where high purity helium (Airgas) with a constant flow pressure of 12 psi was used as the carrier gas. The temperature of the inlet was set at 225 °C. The GC oven was programmed with the following temperature regime: hold at 35 °C for 2 min, ramp to 50 °C at 5

°C/min, hold at 50 °C for 3 min, ramp to 230 °C at 15 °C/min, and hold at 230 °C for 10 min. The TCD temperature was set at 200 °C, with a reference gas flow rate of 15 mL/min and a makeup gas flow rate of 5 mL/min.

To quantify water vapor, 1 mL of gas phase sample was injected into an Agilent 6890N GC system equipped with a 5975 mass selection detector and a Q-Bond PLOT column (Restek). The helium carrier gas was set at a constant flow rate of 3 mL/min. The temperature of the inlet was set at 250 °C. The GC oven was programmed with the following temperature regime: start at 35 °C, ramp to 50 °C at 15 °C/min, ramp to 100 °C at 5 °C/min, hold at 100 °C for 3 min, ramp to 250 °C at 25 °C/min, and hold at 250 °C for 4 min.

To quantify light hydrocarbons ($< C_9$) in the gas phase, 1 mL of gas phase sample was injected into the Agilent 7820A GC equipped with a flame ionization detector (FID) and the Q-Bond PLOT column (Restek). The helium carrier gas was set at a constant pressure of 15 psi. The temperature of the inlet was set at 250 °C. The GC oven was programmed with the following temperature regime: start at 35 °C, ramp to 50 °C at 15 °C/min, ramp to 100 °C at 5 °C/min, hold at 100 °C for 3 min, ramp to 250 °C at 25 °C/min, and hold at 250 °C for 4 min. The FID temperature was set at 300 °C, with a hydrogen gas flow rate of 30 mL/min and a air flow rate of 400 mL/min.

Finally, to quantify liquid phase products in the condenser, 15 mL of dichloromethane was used to extract these species, and 5-10 mg of biphenyl was added into the solution as a calibration standard. 5 μL of solution was injected into the the Agilent 7820A GC equipped with the FID using a

Rxi®-5Sil MS capillary column. The helium carrier gas was set at a constant pressure of 5 psi and a split ratio of 10. The temperature of the inlet was set at 300 °C. The GC oven was programmed with the following temperature regime: hold at 30 °C for 5 min, ramp to 180 °C at 7.5 °C/min, hold at 180 °C for 5 min, ramp to 285 °C at 15 °C/min, and hold at 285 °C for 8 min. The FID temperature was set at 300 °C, with a hydrogen gas flow rate of 30 mL/min and a air flow rate of 400 mL/min.

3. Results and discussion

3.1. Sample morphology

In Figure 2 we show images and scanning electron micrographs (SEM) of PICA, in its virgin and charred forms. The virgin material (Figure 2a), extracted from a billet of the material supplied by FMI, presents the typical yellowish color resulting from curing of the resin during manufacturing, while the charred sample (Figure 2b), generated from pyrolysis experiments after heating in inert atmosphere at 1250 K, has the typical dark color of a carbonized compound. The micrographs of the virgin material (Figures 2a' and a") show the highly porous phenolic matrix, dispersed in between the fibrous network and deposited on the carbon fibers.

The highly porous architecture of the nano-dispersed phenolic is responsible for adsorption of atmospheric moisture [22, 23]. Changes in water phase within PICA are considered to have affected the response of in-depth temperature sensors in the PICA heat shield during the early phase of MSL entry [22, 23]. For the charred material, shown in the micrographs in Figures 2b' and b", the matrix is converted into a thin carbonaceous phase in between

and on the fibers after pyrolysis.

3.2. Sample mass loss

Figure 3 displays the percent mass loss of PICA as a function of temperature measured with the electronic balance and quantified by the GC. The mass loss from PICA pyrolysis is compared to that from resole PF resin pyrolysis obtained in our previous experiments [11]. It can be shown that the mass loss of PICA is approximately half of the mass loss of PF resin. Since phenolic resin consists of approximately half of the PICA mass, given that the carbon preform does not undergo mass loss during pyrolysis, the estimated amount of the initial phenolic resin mass loss in PICA due to pyrolysis is close to the mass loss of resole PF.

The cumulative mass loss of PICA as a function of temperature is shown in Figure 4. As illustrated in the figure, at a reaction temperature above 1250 K, about 19% of the initial PICA mass was lost by pyrolysis. A similar value (17%) was also obtained from thermo-gravimetric analysis (TGA), where a SEIKO SSC/5200 TG/DTA220 thermal analysis station was used to test approximately 2.2 mg of PICA sample in an alumina pan at a heating rate of 10 K/min from room temperature to approximately 1250 K. Prior to the measurement, the chamber was evacuated and filled with argon up to room atmosphere. During the heating, a constant flow of argon at 40 ml/min was supplied.

Figures 3 and 4 show that the total mass of the pyrolysis products quantified by the GC was very close to the total mass loss measured by the balance. This suggests that our GC analysis has captured a majority, if not all, of the species produced from the pyrolysis of PICA and resole PF resins.

3.3. Reaction pressure

Figure 5 shows final reactor pressure measured at room temperature after each PICA pyrolysis step, an indication of pyrolysis gas molar yields (as opposed to mass yields). The results are also compared against those obtained in our previous resole PF pyrolysis experiments. As depicted in the figure, the final reactor pressure increased with respect to pyrolysis temperature under 900 K and dropped afterwards. This temperature is higher than the temperature corresponding to the maximum mass loss at approximately 770 K (Figure 3). The higher molar yields with smaller mass loss at higher pyrolysis temperatures suggests that smaller species, such as permanent gases, were formed in this temperature range.

3.4. Species yields

Although mass loss of PICA during pyrolysis behaves similarly to that of PF resin, different degradation pathways may exist due to the presence of carbon preform, different morphology, and, possibly, different level of cross-linking, affecting the distributions of different pyrolysis products. Detailed quantification of species production using GC was thus performed to provide detailed kinetics during PICA pyrolysis. Figure 6 displays the percent mass loss of PICA quantified by GC, where major pyrolysis products are grouped into three families: water, volatile species (phenol derivatives and aromatics), and permanent gases (H_2, CO, CO_2, and CH_4). It is shown that water is one of the main products during pyrolysis throughout the entire temperature range. Volatile compounds are produced between 600 and 1050 K, with residual traces up to 1250 K. Permanent gases were detected between 650 and 1250 K, with the majority being produced between 700 and 1050 K.

This product distribution, with a mass production peak at a temperature of approximately 770 K, follows the well known three-step pyrolysis mechanism described by Trick et al. [18, 19].

Detailed distributions of pyrolysis products from PICA pyrolysis are further compared to those from resole PF resin pyrolysis obtained previously [11] in the following subsections. The molar production results reported here were normalized on the basis of 100 mg of PICA samples and 50 mg of resole PF samples for comparison.

3.4.1. Water and permanent gases

The amount of water vapor and permanent gases produced from PICA pyrolysis are compared with those from resole PF resin pyrolysis in Figure 7. As illustrated in the figure, water vapor was detected at all temperatures. Permanent gases, including H_2, CH_4, CO, and CO_2, become dominant at pyrolysis temperatures above 800 K. Hydrogen has the highest molar yields, followed by CO and CH_4. Little but noticeable yields of CO_2 were detected.

The temperature dependence of water and permanent gas production were found to be similar between resole PF resin pyrolysis (Figure 7a) and PICA pyrolysis (Figure 7b). However, three differences were observed: 1) the amount of hydrogen produced during PICA pyrolysis was found to be a factor of 5 lower than that produced during resole PF resin pyrolysis; 2) water was detected throughout the whole temperature range during PICA pyrolysis, as opposed to only below 850 K during resole PF resin pyrolysis; 3) slightly lower methane yields were found from PICA pyrolysis. It is believed that water produced below 850 K comes from the condensation reaction between two hydroxyl (-OH) groups during phenolic resin pyrolysis [9, 18, 19].

The origin of water above 850 K during PICA pyrolysis is less certain. One likely contribution is secondary decomposition reactions of phenol derivatives produced from direct PICA pyrolysis, catalyzed by carbon preform (see discussion in the next subsection). Another possible pathway is reverse water gas shift reaction, where high temperature favors the conversion of hydrogen and carbon dioxide into water and carbon monoxide in the presence of catalysts [24]. Finally, despite our best effort to keep the samples in vacuum environment, there is unavoidable ambient air leaking into the system at room temperature between runs, causing small but noticeable amount of ambient water trapped in the charred pyrolyzed samples.

3.4.2. Phenol derivatives and aromatics

The production of phenol and its derivatives (i.e., cresol, dimethylphenol, and trimethylphenol) from PICA pyrolysis is compared to that from resole PF resin pyrolysis in Figure 8. About half of the phenol and cresol were measured during PICA pyrolysis compared to resole PF resin pyrolysis, while the yields of dimethylphenol were found to be similar. A comparison of the aromatics (i.e., benzene, toluene, and xylene) produced from the two reactions, shown in Figure 9, reveals that aromatic yields were generated at temperatures between 800 and 1000 K during PICA pyrolysis. In contrast, aromatics production is concentrated in the 750–850 K range for resole PF resin pyrolysis. This difference suggests that at high reaction temperatures (> 800 K), cleavage reactions may be catalyzed by carbon preform to produce benzene and toluene from phenol and cresol [25]. The removal of hydroxyl (-OH) groups from phenol and cresol may also contribute to the higher water yields in this temperature range, as discussed earlier.

3.4.3. Light hydrocarbons

The amount of light hydrocarbons (C_2H_4, C_2H_6, C_3H_6, C_3H_8) produced from resole PF resin pyrolysis and PICA pyrolysis is compared in Figure 10. Note that light hydrocarbons have substantially lower yields compared to other product families such as water vapor, permanent gases, phenol derivatives, and aromatics. As discussed in our previous work, these species are likely produced from recombination of small hydrocarbon radicals in the colder zones of our reactor system. The yields of light hydrocarbons from PICA pyrolysis were observed to be lower than those from resole PF resin pyrolysis, suggesting that carbon preform in PICA may scavenge the hydrocarbon radicals produced during the pyrolysis and charring process.

The molar yields of pyrolysis products at each pyrolysis temperature are summarized in Tables 1. These quantitative PICA pyrolysis data can be utilized for the development of a detailed chemical kinetic pyrolysis model for material response codes for accurate predictions of PICA degradation.

4. Conclusions

Batch pyrolysis of PICA was performed using a step-wise heating procedure in 50 K increments from room temperature up to 1250 K. Approximately 100 mg of PICA sample was loaded in a reactor assembly that allowed to quantify yields of pyrolysis products by means of gas chromatography techniques. Key observations from our experiments include:

- Mass loss of PICA pyrolysis peaks at ≈770 K, similar to that of resole PF resin pyrolysis. The pyrolysis of PICA also follows the well-known three step phenol-formaldehyde resin pyrolysis mechanism.

- The cumulative mass loss of PICA reaches ≈19% after 1250 K.

- Water vapor was detected at all reaction temperatures, as opposed to only below 850 K for resole PF resin pyrolysis. Water vapor produced above 850 K may be from desorption of ambient humidity trapped in the samples between runs, suggesting high char content in the pyrolyzed PICA samples, or from the removal of hydroxyl groups from phenol and cresol assisted by carbon preform during pyrolysis.

- Hydrogen yields from PICA pyrolysis are approximately one-fifth of those from resole PF resin pyrolysis.

- Phenol and cresol yields from PICA pyrolysis are lower than those from resole PF resin pyrolysis, whereas benzene and toluene yields from PICA pyrolysis are higher than those from resole PF resin pyrolysis. This suggests that carbon preform facilitates phenol and cresol cleavage to produce benzene and toluene.

- Light hydrocarbon yields from PICA pyrolysis are lower than those from resole PF resin pyrolysis, suggesting that carbon preform may react with light hydrocarbon radicals during charring.

The differences in product distributions between PICA and resole PF resin pyrolysis suggest that the microstructure and chemical composition differences in TPS materials would result in distinct material response. This suggests that future studies using state-of-the-art experimental and computational techniques are needed to carefully separate primary substrate pyrolysis reactions and secondary processes such as secondary pyrolysis and gas phase

reactions and diffusion-reaction coupling. This work also stresses the need of performing dedicated pyrolysis-product characterizations for each material of interest and develop a tailored pyrolysis model for material response simulations.

Acknowledgments

This research was originally funded by NASA's Fundamental Aeronautic Program Hypersonics NRA grant NNX12AG47A. It is currently supported by the Space Technology Research Grants Program.

References

[1] M. Stackpoole, S. Sepka, I. Cozmuta, D. Kontinos, Post-flight evaluation of stardust sample return capsule forebody heatshield material, AIAA Paper 2008-1202.

[2] Pica heat shield.
URL http://www.spacex.com/news/2013/04/04/pica-heat-shield

[3] H. Ritter, P. Portela, K. Keller, J. M. Bouilly, S. Burnage, Development of a european ablative material for heatshields of sample return missions, 6th European Workshop on TPS and Hot structures, Stuttgart, Germany, 1-3 April 2009.

[4] Y.-K. Chen, F. Milos, Effects of non-equilibrium chemistry and darcy-forchheimer flow of pyrolysis gas for a charring ablator, AIAA paper 2011-3122.

[5] A. Martin, I. Boyd, M. W. Wright, I. Cozmuta, Chemistry model for ablating carbon-phenolic material during atmospheric re-entry, AIAA Paper 2010-1175.

[6] J. Lachaud, I. Cozmuta, N. N. Mansour, Multiscale approach to ablation modeling of phenolic impregnated carbon ablators, Journal of Spacecraft and Rockets 47 (6) (2010) 910–921.

[7] J. Lachaud, N. N. Mansour, Porous-material analysis toolbox based on openfoam and applications, Journal of Thermophysics and Heat Transfer 28 (2) (2014) 191–202.

[8] J. Lachaud, T. van Eekelen, J. B. Scoggins, T. E. Magin, N. N. Mansour, Detailed chemical equilibrium model for porous ablative materials, International Journal of Heat and Mass Transfer 90 (2015) 1034–1045.

[9] B. K. Bessire, S. A. Lahankar, T. K. Minton, Pyrolysis of phenolic impregnated carbon ablator (pica), ACS Applied Materials and Interfaces 7 (3) (2015) 1383–1395.

[10] H.-W. Wong, J. Peck, R. A. Edwards, G. Reinisch, J. Lachaud, N. N. Mansour, Measurement of pyrolysis products from phenolic polymer thermal decomposition, AIAA Paper 2014-1388.

[11] H.-W. Wong, J. Peck, R. E. Bonomi, J. Assif, F. Panerai, G. Reinisch, J. Lachaud, N. N. Mansour, Quantitative determination of species production from phenol-formaldehyde resin pyrolysis, Polymer Degradation and Stability 112 (2015) 122–131.

[12] H.-W. Wong, J. Peck, J. Assif, J. Lachaud, N. N. Mansour, Quantitative determination of species production from the pyrolysis of the phenolic impregnated carbon ablator (pica), AIAA Paper 2015-1447.

[13] R. W. Pike, G. C. April, E. G. del Valle, Non-equilibrium flow and the kinetics of chemical reactions in the char zone, Status report - grant number 19-001-016, NASA (1967).

[14] G. F. Sykes, Decomposition characteristics of a char-forming phenolic polymer used for ablative composites, Technical report, NASA (1967).

[15] G. C. April, Energy transfer in the char zone of a charring ablator, PhD thesis, Louisiana State University, also, NASA CR 107533. (1969).

[16] H. W. Goldstein, Pyrolysis kinetics of nylon 6-6, phenolic resin, and their composites, Journal of Macromolecular Science, Part A 3 (4) (1969) 649–673.

[17] G. F. Sykes, Thermal cracking of phenolic-nylon pyrolysis products on passing through a heated char, Technical report, NASA (1970).

[18] K. A. Trick, T. E. Saliba, Mechanisms of the pyrolysis of phenolic resin in a carbon/phenolic composite, Carbon 33 (11) (1995) 1509–1515.

[19] K. A. Trick, T. E. Saliba, S. S. Sandhu, A kinetic model of the pyrolysis of phenolic resin in a carbon/phenolic composite, Carbon 35 (3) (1997) 393–401.

[20] N. N. Mansour, J. Lachaud, T. E. Magin, J. de Muelenaere, Y.-K.

Chen, High-fidelity charring ablator thermal response model, AIAA Paper 2011-3124.

[21] H. K. Tran, C. E. Johnson, D. J. Rasky, F. C. L. Hui, M.-T. Hsu, T. Chen, Y. K. Chen, D. Paragas, L. Kobayashi, Phenolic impregnated carbon ablators (pica) as thermal protection systems for discovery missions, Tech. Rep. 110440, NASA Technical Memorandum (1997).

[22] A. D. Omidy, F. Panerai, J. R. Lachaud, N. N. Mansour, A. Martin, Effects of water phase change on the material response of low-density carbon-phenolic ablators, in press, Journal of Thermophysics and Heat Transfer.

[23] D. L. Smith, A. D. Omidy, H. Weng, T. R. White, A. Martin, Effects of water presence on low temperature phenomenon in porous tps materials, AIAA Paper 2015-2505.

[24] C. Ratnasamy, J. P. Wagner, Water gas shift catalysis, Catalysis Reviews 51 (3) (2009) 325–440.

[25] K. Brezinsky, M. Pecullan, I. Glassman, Pyrolysis and oxidation of phenol, Journal of Physical Chemistry A 102 (44) (1998) 8614–8619.

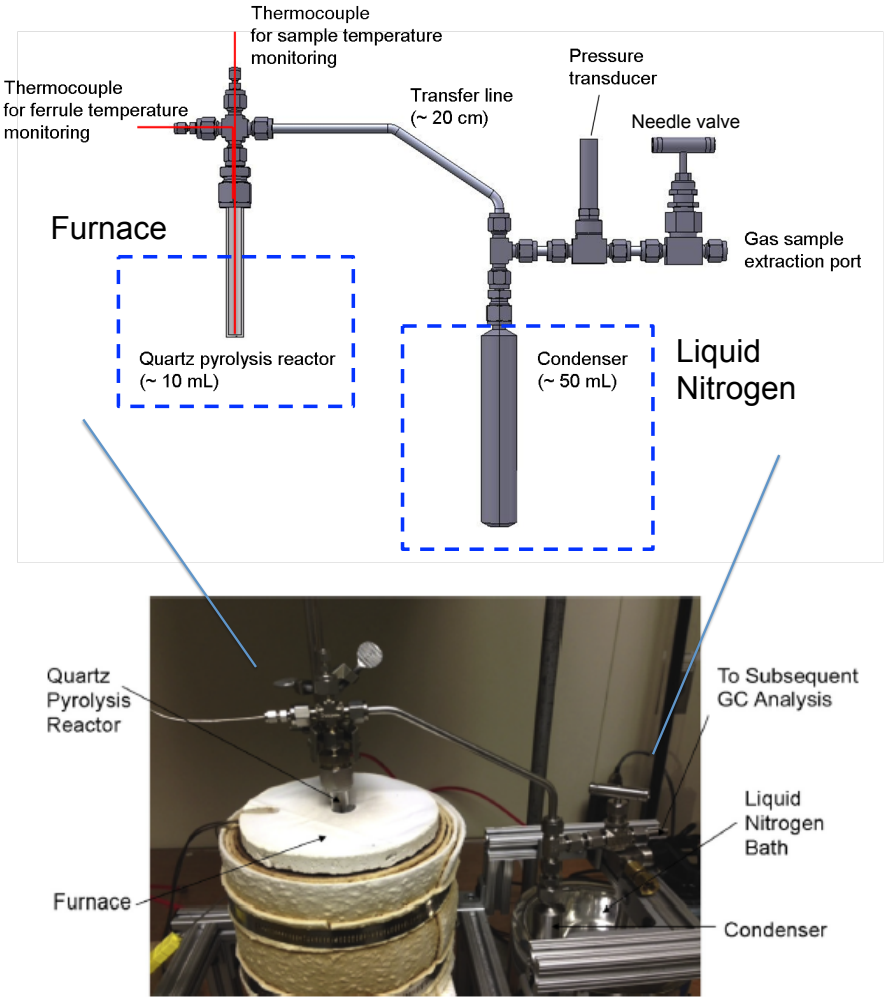

Figure 1: The batch reactor system used in this study.

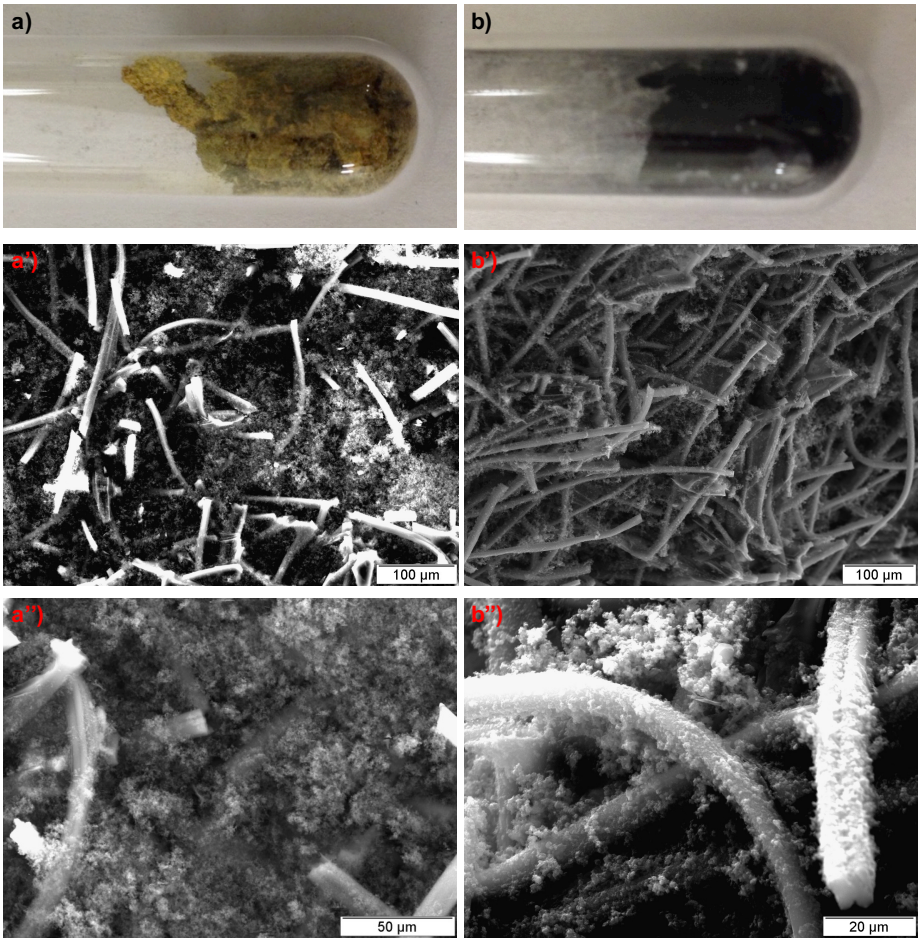

Figure 2: (a) Virgin PICA sample, b) charred PICA sample, a',a''') micrographs of virgin PICA at different magnifications, and b'b") micrographs of virgin PICA at different magnifications.

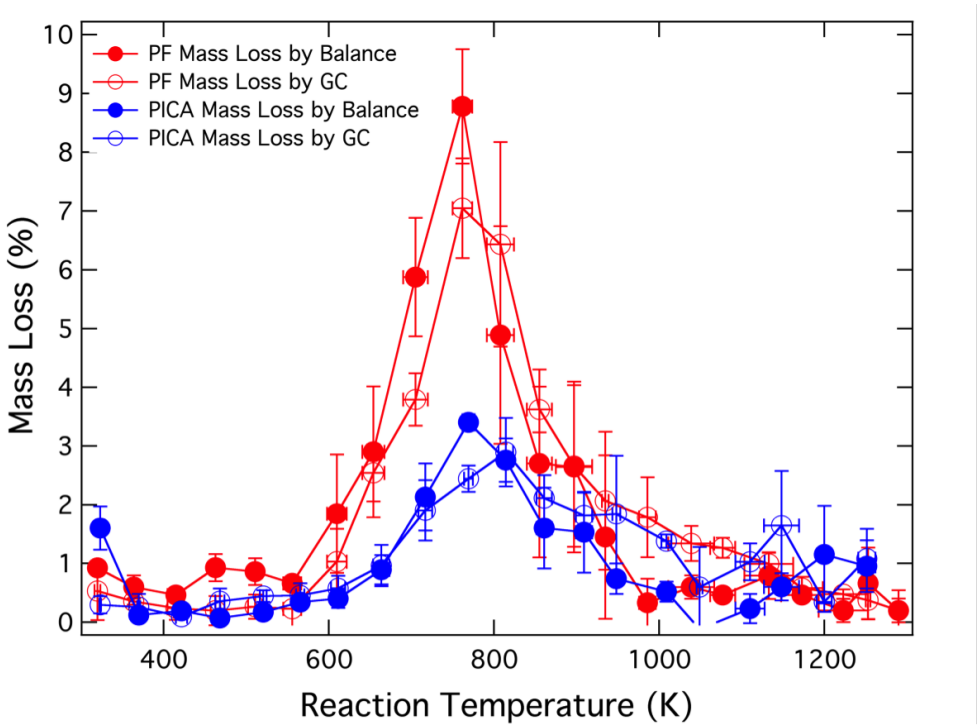

Figure 3: Comparison of mass loss from resole PF pyrolysis [11] and PICA pyrolysis measured with balance and quantified by GC.

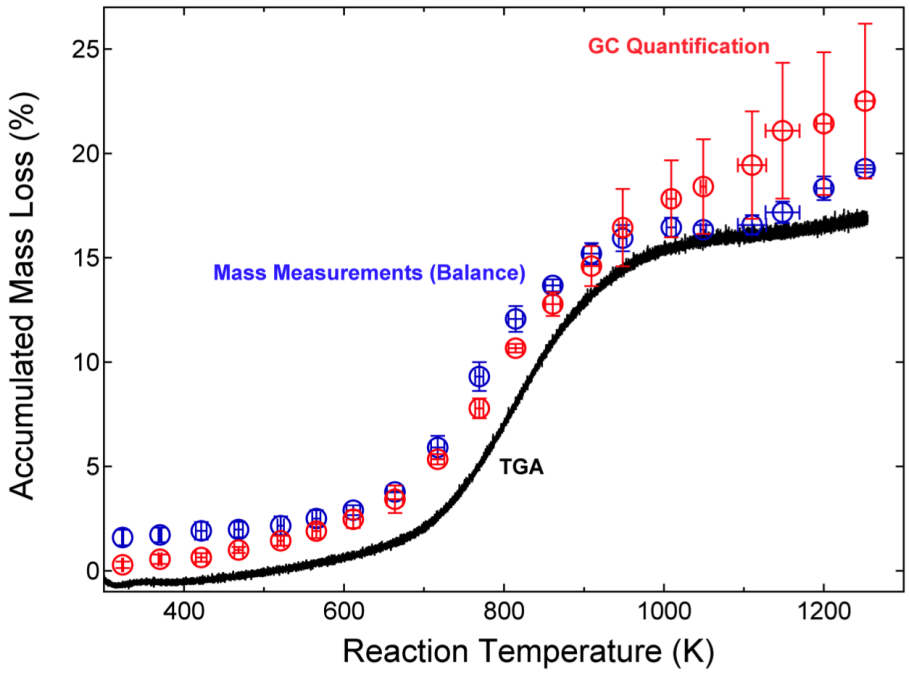

Figure 4: The cumulated mass loss of PICA pyrolysis measured by the balance, GC, and TGA.

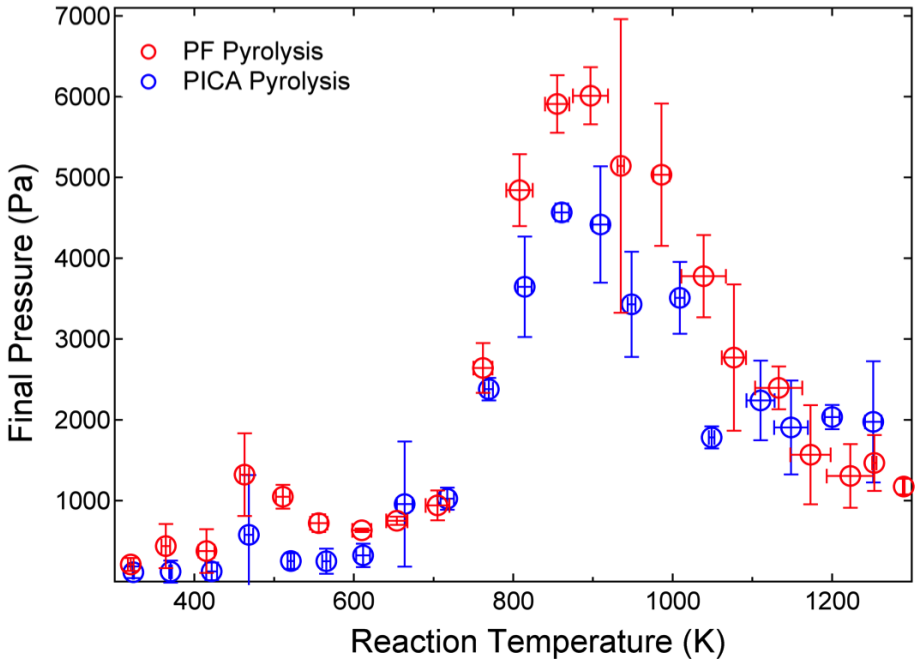

Figure 5: The final pressure measured at room temperature after each run as a function of reaction temperature.

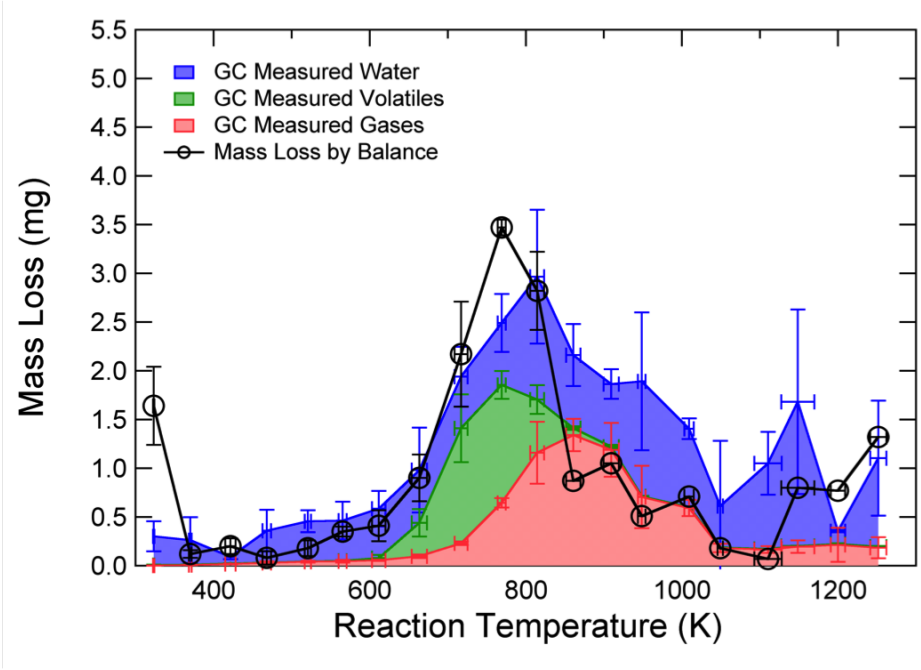

Figure 6: The percent mass loss as a function of reaction temperature from PICA pyrolysis.

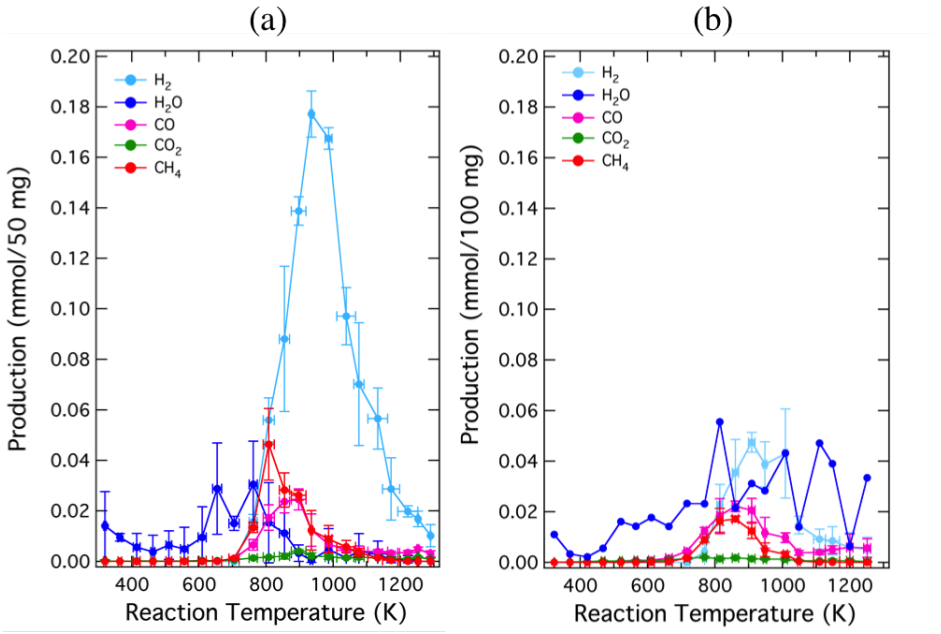

Figure 7: The amount of water and permanent gases produced as a function of reaction temperature during (a) resole PF resin pyrolysis and (b) PICA pyrolysis.

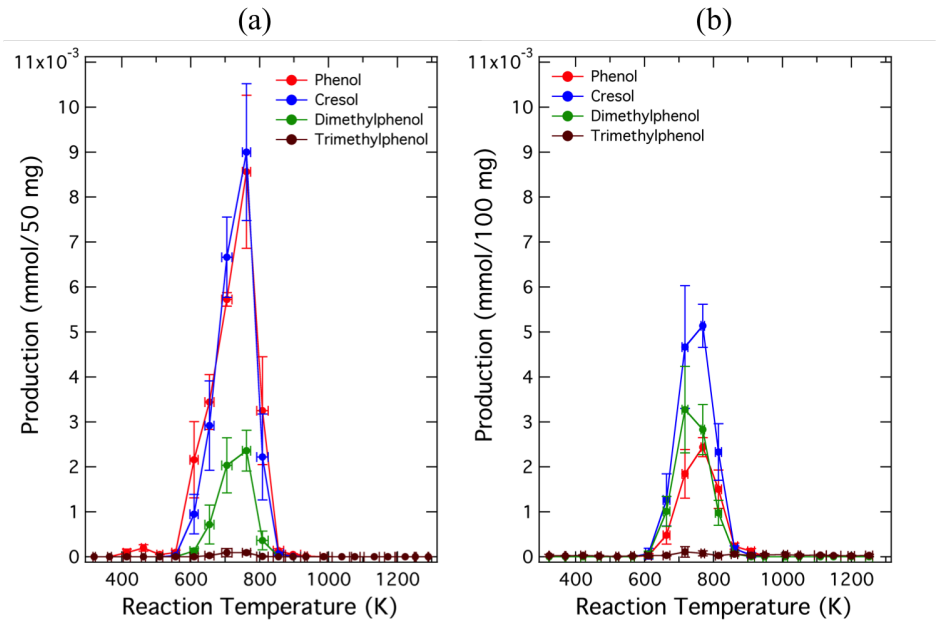

Figure 8: The amount of phenol and its derivatives produced as a function of reaction temperature during (a) resole PF resin pyrolysis and (b) PICA pyrolysis.

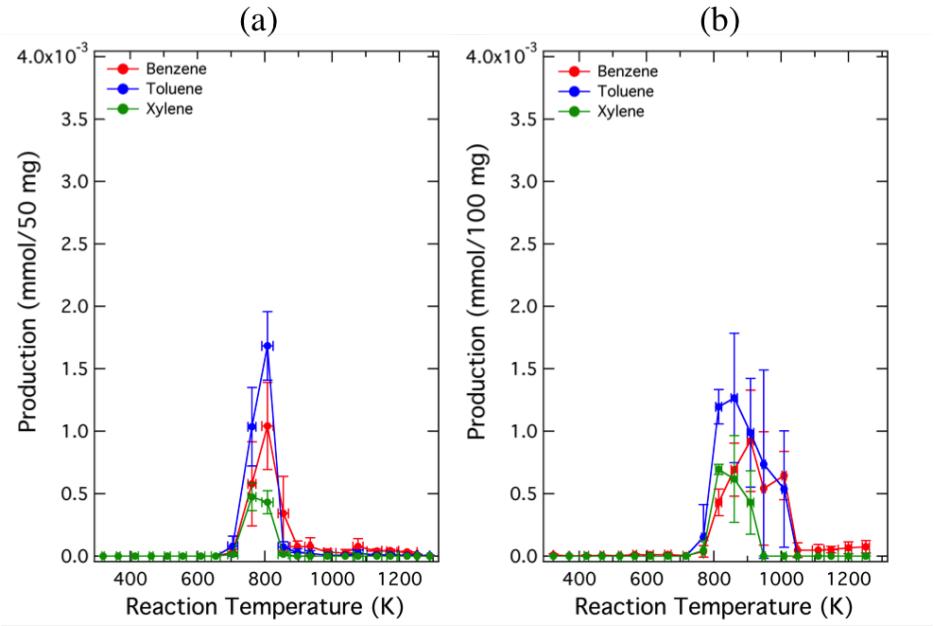

Figure 9: The amount of aromatics produced as a function of reaction temperature during (a) resole PF resin pyrolysis and (b) PICA pyrolysis.

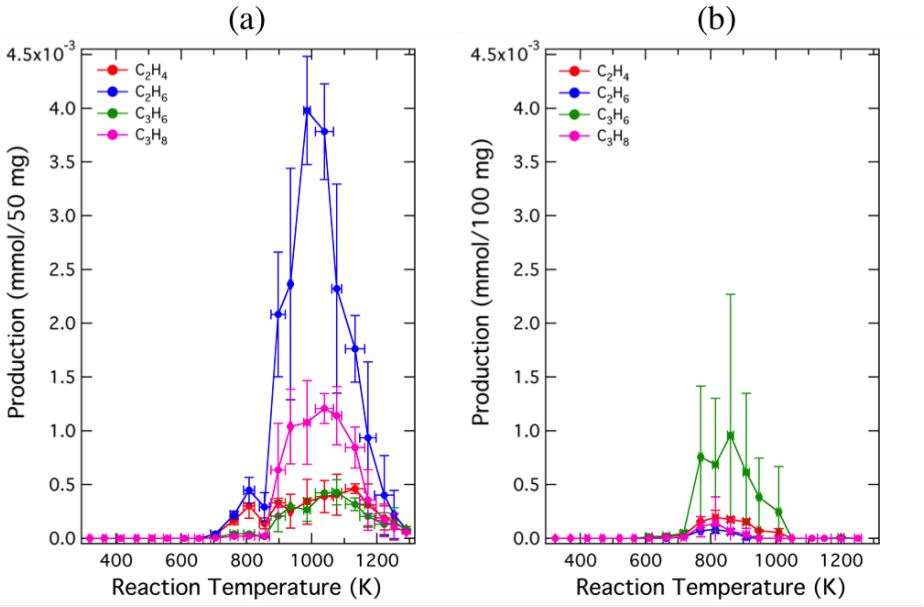

Figure 10: The amount of light hydrocarbons produced as a function of reaction temperature from (a) resole phenolic pyrolysis and (b) PICA pyrolysis.

Pyrolysis	Molar yields (mmol/100 mg PICA) – permanent gases				
temperature (K)	H_2O	H_2	CH_4	CO	CO_2
323	$1.79 \cdot 10^{-2}$				$7.19 \cdot 10^{-5}$
370	$1.37 \cdot 10^{-2}$			$1.45 \cdot 10^{-5}$	$1.64 \cdot 10^{-4}$
422	$4.92 \cdot 10^{-3}$			$6.94 \cdot 10^{-5}$	$3.57 \cdot 10^{-4}$
468	$2.26 \cdot 10^{-2}$			$1.99 \cdot 10^{-4}$	$5.24 \cdot 10^{-4}$
521	$2.53 \cdot 10^{-2}$			$6.15 \cdot 10^{-4}$	$5.37 \cdot 10^{-4}$
565	$2.78 \cdot 10^{-2}$		$1.24 \cdot 10^{-5}$	$7.53 \cdot 10^{-4}$	$5.52 \cdot 10^{-4}$
612	$3.84 \cdot 10^{-2}$		$1.47 \cdot 10^{-4}$	$8.99 \cdot 10^{-4}$	$6.09 \cdot 10^{-4}$
664	$3.23 \cdot 10^{-2}$		$3.07 \cdot 10^{-4}$	$1.70 \cdot 10^{-3}$	$9.43 \cdot 10^{-4}$
717	$3.20 \cdot 10^{-2}$		$1.77 \cdot 10^{-3}$	$4.43 \cdot 10^{-3}$	$1.58 \cdot 10^{-3}$
769	$5.03 \cdot 10^{-2}$	$4.28 \cdot 10^{-3}$	$8.95 \cdot 10^{-3}$	$1.24 \cdot 10^{-2}$	$2.06 \cdot 10^{-3}$
814	$7.67 \cdot 10^{-2}$	$2.28 \cdot 10^{-2}$	$1.63 \cdot 10^{-2}$	$1.86 \cdot 10^{-2}$	$1.43 \cdot 10^{-3}$
861	$4.08 \cdot 10^{-2}$	$3.56 \cdot 10^{-2}$	$1.72 \cdot 10^{-2}$	$2.22 \cdot 10^{-2}$	$1.86 \cdot 10^{-3}$
909	$3.59 \cdot 10^{-2}$	$4.75 \cdot 10^{-2}$	$1.24 \cdot 10^{-2}$	$2.05 \cdot 10^{-2}$	$1.42 \cdot 10^{-3}$
948	$6.66 \cdot 10^{-2}$	$3.87 \cdot 10^{-2}$	$4.98 \cdot 10^{-3}$	$1.16 \cdot 10^{-2}$	$1.37 \cdot 10^{-3}$
1009	$6.22 \cdot 10^{-2}$	$4.32 \cdot 10^{-2}$	$3.23 \cdot 10^{-3}$	$9.78 \cdot 10^{-3}$	$1.25 \cdot 10^{-3}$
1049	$3.92 \cdot 10^{-2}$	$1.47 \cdot 10^{-2}$	$4.63 \cdot 10^{-4}$	$3.76 \cdot 10^{-3}$	$6.38 \cdot 10^{-4}$
1110	$5.37 \cdot 10^{-2}$	$9.22 \cdot 10^{-3}$	$1.07 \cdot 10^{-4}$	$3.96 \cdot 10^{-3}$	$6.59 \cdot 10^{-4}$
1148	$8.38 \cdot 10^{-2}$	$8.61 \cdot 10^{-3}$	$4.28 \cdot 10^{-5}$	$5.01 \cdot 10^{-3}$	$7.28 \cdot 10^{-4}$
1200	$1.95 \cdot 10^{-2}$	$5.88 \cdot 10^{-3}$		$5.94 \cdot 10^{-3}$	$6.73 \cdot 10^{-4}$
1252	$5.37 \cdot 10^{-2}$	$5.14 \cdot 10^{-3}$		$5.64 \cdot 10^{-3}$	$2.85 \cdot 10^{-4}$
Total	$7.97 \cdot 10^{-1}$	$2.36 \cdot 10^{-1}$	$6.60 \cdot 10^{-2}$	$1.28 \cdot 10^{-1}$	$1.77 \cdot 10^{-2}$

Pyrolysis	Molar yields (mmol/100 mg PICA) – phenol derivatives and aromatics						
temperature (K)	C_6H_6O	C_7H_8O	$C_8H_{10}O$	$C_9H_{12}O$	C_6H_6	C_7H_8	C_8H_{10}
323					$9.77 \cdot 10^{-6}$		
370					$2.27 \cdot 10^{-6}$		
422					$3.36 \cdot 10^{-6}$		
468					$5.49 \cdot 10^{-6}$		
521					$4.86 \cdot 10^{-6}$		
565					$1.24 \cdot 10^{-5}$		
612	$2.67 \cdot 10^{-5}$	$7.04 \cdot 10^{-5}$	$4.59 \cdot 10^{-5}$		$1.12 \cdot 10^{-5}$		
664	$4.83 \cdot 10^{-4}$	$1.27 \cdot 10^{-3}$	$1.02 \cdot 10^{-3}$		$1.25 \cdot 10^{-5}$		
717	$1.85 \cdot 10^{-3}$	$4.68 \cdot 10^{-3}$	$3.28 \cdot 10^{-3}$	$1.07 \cdot 10^{-4}$	$3.51 \cdot 10^{-6}$		
769	$2.44 \cdot 10^{-3}$	$5.13 \cdot 10^{-3}$	$2.82 \cdot 10^{-3}$	$7.45 \cdot 10^{-5}$	$3.82 \cdot 10^{-5}$	$1.54 \cdot 10^{-4}$	$4.69 \cdot 10^{-5}$
814	$1.50 \cdot 10^{-3}$	$2.32 \cdot 10^{-3}$	$9.74 \cdot 10^{-4}$		$4.32 \cdot 10^{-4}$	$1.20 \cdot 10^{-3}$	$6.94 \cdot 10^{-4}$
861	$2.33 \cdot 10^{-4}$	$1.83 \cdot 10^{-4}$	$6.41 \cdot 10^{-5}$		$6.91 \cdot 10^{-4}$	$1.26 \cdot 10^{-3}$	$6.14 \cdot 10^{-4}$
909	$1.25 \cdot 10^{-4}$	$3.21 \cdot 10^{-5}$			$9.18 \cdot 10^{-4}$	$9.83 \cdot 10^{-4}$	$4.27 \cdot 10^{-4}$
948					$5.36 \cdot 10^{-4}$	$7.27 \cdot 10^{-4}$	
1009					$6.47 \cdot 10^{-4}$	$5.32 \cdot 10^{-4}$	
1049					$4.80 \cdot 10^{-5}$		
1110					$4.84 \cdot 10^{-5}$		
1148					$5.20 \cdot 10^{-5}$		
1200					$6.57 \cdot 10^{-5}$		
1252					$7.38 \cdot 10^{-5}$		
Total	$6.65 \cdot 10^{-3}$	$1.37 \cdot 10^{-2}$	$8.20 \cdot 10^{-3}$	$1.82 \cdot 10^{-4}$	$3.62 \cdot 10^{-3}$	$4.85 \cdot 10^{-3}$	$1.78 \cdot 10^{-3}$

Pyrolysis	Molar yields (mmol/100 mg PICA) – light hydrocarbons			
temperature (K)	C_2H_4	C_2H_6	C_3H_6	C_3H_8
323				
370				
422				
468				
521				
565				
612			$1.39 \cdot 10^{-5}$	
664	$1.84 \cdot 10^{-5}$		$2.12 \cdot 10^{-5}$	$7.04 \cdot 10^{-6}$
717	$3.07 \cdot 10^{-5}$	$1.32 \cdot 10^{-5}$	$4.69 \cdot 10^{-5}$	$9.92 \cdot 10^{-6}$
769	$1.56 \cdot 10^{-4}$	$7.20 \cdot 10^{-5}$	$7.49 \cdot 10^{-4}$	$1.07 \cdot 10^{-4}$
814	$1.95 \cdot 10^{-4}$	$8.13 \cdot 10^{-5}$	$6.78 \cdot 10^{-4}$	$1.44 \cdot 10^{-4}$
861	$1.74 \cdot 10^{-4}$	$6.15 \cdot 10^{-5}$	$9.47 \cdot 10^{-4}$	$6.96 \cdot 10^{-5}$
909	$1.53 \cdot 10^{-4}$	$9.85 \cdot 10^{-6}$	$6.10 \cdot 10^{-4}$	$3.48 \cdot 10^{-5}$
948	$6.94 \cdot 10^{-5}$		$3.80 \cdot 10^{-4}$	
1009	$5.55 \cdot 10^{-5}$		$2.44 \cdot 10^{-4}$	
1049				
1110				
1148				
1200			$6.12 \cdot 10^{-6}$	
1252				
Total	$8.51 \cdot 10^{-4}$	$2.38 \cdot 10^{-4}$	$3.69 \cdot 10^{-3}$	$3.72 \cdot 10^{-4}$

Table 1: Molar yields of pyrolysis products versus pyrolysis temperature.